Topics in Catalysis (2018) 61:1624–1632
https://doi.org/10.1007/s11244-018-1008-0

ORIGINAL PAPER

Enhanced Stability and Propene Yield in Propane Dehydrogenation on PtIn/Mg(Al)O Catalysts with Various In Loadings

Weerachon Tolek[1] · **Kongkiat Suriye**[2] · **Piyasan Praserthdam**[1] · **Joongjai Panpranot**[1]

Abstract

The dehydrogenation of propane on In-promoted Pt (0.3 wt% Pt) supported on hydrotalcite Mg(Al)O with different In loadings (0.2–1.0 wt% In) was investigated at 550 °C atmospheric pressure. All the bimetallic PtIn/Mg(Al)O showed higher propane conversion and propene selectivity than the Pt/Mg(Al)O with Pt0.8In exhibited the best catalytic performances with 97.5% propylene selectivity and 27.5% yield after 5 h time-on-stream. The addition of In to the monometallic Pt catalyst could reduce the acidity strength especially the strong acid site. As revealed by the H_2-TPR and XPS results, addition of In by impregnation on Pt/Mg(Al)O also led to the formation of metallic In and PtIn alloy, which greatly enhanced the catalyst activity and reduced coke formation on the support. Nevertheless, excessive In loading (i.e., Pt1.0In) resulted in a descending trend of catalyst activity compared to the Pt0.8In, due probably to the large amount of metallic In being formed, which was disadvantageous in propane dehydrogenation.

Keywords Propane dehydrogenation · Hydrotalcite · PtIn bimetallic catalyst · XPS · Indium

1 Introduction

Propylene is an important feedstock in petrochemical industry for the production of a wide variety of chemicals and polymers such as polypropylene, acrolein, acrylic acid and oligomers [1, 2]. The commercial methods for producing the light olefins are steam cracking of alkanes, naphtha, or gas oil but the process is highly endothermic, which usually requires high temperature to obtain a high yield of olefins. The catalytic dehydrogenation of light paraffins is an alternative route for the production of light olefins with improved olefins selectivity and lower coke formation [3–6]. However, side reactions including cracking, hydrogenolysis, isomerization, and oligomerization reactions are commonly found with catalytic dehydrogenation of alkane. Thus, catalyst deactivation due to coke formation is inevitable under the reaction conditions used.

Support bimetallic Pt-based catalysts are important for many hydrocarbon transformation reactions. Pt–Sn/Al_2O_3 has been used extensively as a well-known catalyst for propane dehydrogenation because of their high activity and high selectivity to propylene [7–9]. However, Pt–Sn/Al_2O_3 catalysts must undergo continuous or frequent regeneration to restore the catalytic activity as deactivation due to coking cannot be completely eliminated [10]. Consequently, another promoter including alkali metals (Li, K, Na, Mg), Zn and rare earth metals (La, Ce, Y) has been added to Pt–Sn/Al_2O_3 catalysts to enhance the tolerance against catalyst deactivation. The primary roles of these promoters are to improve the thermal stabilities of supports and to modify the acidic/basic properties of supports and metal–support interactions [11–13]. A number of second metal promoters such as Sn, Zn, Ge, Ga, or In can interact with Pt to form bimetallic alloys [14–18]. PtIn catalysts have been found to be more homogenous in composition than PtSn particles and more stable in alkane dehydrogenation [16, 19].

Mg(Al)O or hydrotalcite has received considerable attention as an efficient support for Pt-based catalysts for light alkane dehydrogenation owing to their moderately basicity, high thermal stability, as well as the capability of enhancing

---

✉ Joongjai Panpranot
joongjai.p@chula.ac.th

[1] Center of Excellence on Catalysis and Catalytic Reaction Engineering, Department of Chemical Engineering, Faculty of Engineering, Chulalongkorn University, Bangkok 10330, Thailand

[2] SCG Chemicals Co., Ltd., 1 Siam-cement Rd, Bang Sue, Bangkok 10800, Thailand

Pt particle dispersion due to the presence of Al cations on the support surface [5, 20–24]. Previous studies have shown that non-acidic supports such as K–L zeolite, alkali-doped alumina, spinels, and calcined Mg(Al)O could minimize the adsorption of ethene and the formation of coke [22, 25, 26].

Due to their promising properties, the combination of PtIn and Mg(Al)O supports has been employed in the recent development of propane dehydrogenation catalysts. The effects of calcination temperature of the Mg(Al)O [27], pH values for the preparation of Mg(Al)O [28], and the Mg/Al molar ratios [29] on the PtIn catalysts supported on Mg(Al)O with 0.6 wt% Pt and 1.5 wt% In loadings were investigated. In addition, the induction and deactivation of catalytic activity of the 0.6%Pt–1.5%In on the optimized Mg(Al)O were related to changes in the metal particle size, the specific surface area, and the crystalline phase of the catalysts during propane dehydrogenation at 620 °C and pressure 0.1 MPa [30]. Propane conversion ranging between 50 and 60% with propene selectivity $\geq 97\%$ were obtained during 12–30 h time-on-stream under the conditions reported. Previous studies by Wu et al. [5] and Sun et al. [31] also reported the effect of bulk In/Pt ratio on Pt/Mg(In)(Al)O catalysts, in which the Mg(In)(Al)O support was prepared by co-precipitation method followed by Pt loading by impregnation and tested in ethane, propane and butane dehydrogenation. However, the characteristics of PtIn/Mg(Al)O with various PtIn compositions and their structural–activity relationship in propane dehydrogenation at relatively lower temperature (i.e., 550 °C) has not yet been clearly demonstrated.

In this study, the Pt–In catalysts supported on a commercially available Mg(Al)O support with the suitable ratio of Mg/Al were prepared with 0.3 wt% Pt and various In loadings from 0.2 to 1.0 wt%. The catalysts were evaluated in propane dehydrogenation at 550 °C under atmospheric pressure. The NH_3-TPD experiments were used to investigate the acid properties of the catalysts. The H_2-temperature programmed reduction (H_2-TPR) and X-ray photoelectron spectroscopy (XPS) measurements were used as primary tools to observe the Pt–In interaction and/or the formation of Pt–In alloys. The types and amount of coke formed on the spent catalysts were also investigated by temperature program oxidation (TPO). The spatial distribution of Pt within the catalysts was observed from the transmission electron microscopy (TEM).

2 Experimental

2.1 Catalyst Preparation

The Pt*x*In catalysts were prepared by the incipient wetness co-impregnation of the calcined commercial hydrotalcite support (Mg/Al = 70:30) with the specific surface area (S_{BET}) about 100 m^2/g. An aqueous solution of chloroplatinic acid hydrate (H_2PtCl_6, Sigma Aldrich) and indium nitrate ($In(NO_3)_3$, Sigma Aldrich) were used as precursor to achieve platinum and indium metal loading for 0.3 and x wt%, where x indicated to indium metal loading ($x = 0.2$–1.0 wt%). The catalysts were dried at room temperature for 2 h and then 110 °C for overnight. After drying, the catalysts were calcined in air flow at 550 °C for 3 h.

2.2 Catalyst Characterization

The acidic properties of the catalysts were analyzed using a Micromeritic Chemisorb 2750 apparatus. Prior to NH_3 adsorption, 0.1 g sample was pretreated at 500 °C for 1 h under He flow (25 cm^3/min). After cooling to 40 °C, NH_3 was adsorbed using a flow of 15 vol % NH_3/He (20 cm^3/min) for 0.5 h. The NH_3 desorption was performed in He (20 cm^3/min) with a heating rate of 10 °C/min and the NH_3 desorption profiles were registered with a thermal conductivity detector. The reducibility and reduction behavior of the prepared catalysts were investigated by H_2-TPR. The sample was pretreated under Ar flow at 500 °C for 1 h to remove a moisture, then being cooled down to temperature at 50 °C. Subsequently, the TPR profiles were recorded under the 10% H_2/Ar flow from 50 to 800 °C with a heating rate of 10 °C/min. The amount of hydrogen uptake was determined by measuring the areas of the reduction profiles obtained from a Micromeritic Chemisorb 2750 automated system attached with ChemiSoft TPx software. The surface electronic states of the catalyst samples after reduction were investigated by XPS using an AMICUS X-ray photoelectron spectrometer with a Mg K_α X-ray as a primary excitation and a KRATOS VISION2 software. XPS element spectra were acquired with 0.1 eV energy step at a pass energy of 75 eV. The TEM images of catalysts were carried out by a JEM-2010 microscope operated at 200 kV. The reduced samples were dispersed in ethanol by ultrasonic, and then a small drop of this solution was placed onto carbon film coated copper grids and dried before testing. Coke formation was determined by the TPO experiments. Approximately 0.3 g of spent catalyst was placed in the quartz tube. The 1% oxygen in helium gas mixture was passed through the system at a flow rate of 25 cm^3/min. The temperature was raised to 700 °C with a heating rate of 5 °C/min. The effluent stream was sampled every 5 min on-line using an Shimadzu GC-2014 gas chromatograph equipped with a TCD detector.

2.3 Propane Dehydrogenation Reaction

The dehydrogenation of propane was performed in a fixed bed stainless steel reactor with size of 0.75 in. under atmospheric pressure. Approximately 2 g of catalyst was placed in the stainless-steel reactor and reduced under H_2 flow

($50\ cm^3/min$) balanced with N_2 ($50\ cm^3/min$) at 550 °C for 1 h followed by purging for 30 min in N_2 to remove the H_2. Subsequently, pure propane in gas phase was fed into the reactor at 20 cm^3/min at a reaction temperature 550 °C. The reaction was carried out for 5 h time-on-stream (TOS). The reactants and products were analyzed on-line using an Agilent 7820A gas chromatograph equipped with a packed column HP-PLOT Al_2O_3 "M" deactivated (50 m with 8 µm ID) and a flame ionization detector (FID). The propane conversion and products selectivity were calculated by weight basis using the following equations:

$$C_3H_8\ \text{conversion}\,(\%) = \frac{C_3H_{8in} - C_3H_{8out}}{C_3H_{8in}} \times 100 \tag{1}$$

$$\text{Product i selectivity}\,(\%) = \frac{\text{Product i}_{out}}{C_3H_{8in} - C_3H_{8out}} \times 100 \tag{2}$$

where C_3H_{8in} and C_3H_{8out} represented the contents of propane in feed and effluent gases, respectively. The terms product i_{out} indicated the contents of product i in the effluent gas.

3 Results and Discussion

3.1 The Catalytic Performances of PtxIn Catalysts in Propane Dehydrogenation

The propane dehydrogenation was carried out at 550 °C and atmospheric pressure for 5 h. From Fig. 1, the monometallic Pt catalyst shows very low conversion and poor stability along the 5 h time on stream with the initial and final conversion of 22.9 and 8.4%, respectively. For the series of Pt*x*In catalysts, the initial and final conversion of propane increased monotonically with increasing In loadings from 0.2 to 0.8 wt%. The initial conversion of monometallic Pt was slightly higher than those of the bimetallic Pt0.2In and Pt0.3In due to the undesired side reactions such as cracking and hydrogenolysis. Further increase of In loading to 1 wt% (Pt1.0In), a declining trend for both activity and stability was observed comparing to the Pt0.8In. Thus, In loading 0.8 wt% was the most satisfied for improving the propane conversion, selectivity, and stability of 0.3 wt% Pt catalyst with In/Pt ratio of 2.7. The initial and final propane conversions of the Pt0.8In were 27.5 and 25.4%, respectively, which were very close to the equilibrium conversion of propane dehydrogenation around 30% at 550 °C [32]. The optimized In/Pt ratio 2.7 in this study was close to the In/Pt ratio 2.5 used in the other studies reported in the literature [27–29]. Moreover, the presence of In on Pt catalyst showed higher propene selectivity compared to the monometallic Pt catalyst due to the significantly decrease of the other side reactions, resulting in much lower alkane and C_{5+} formation.

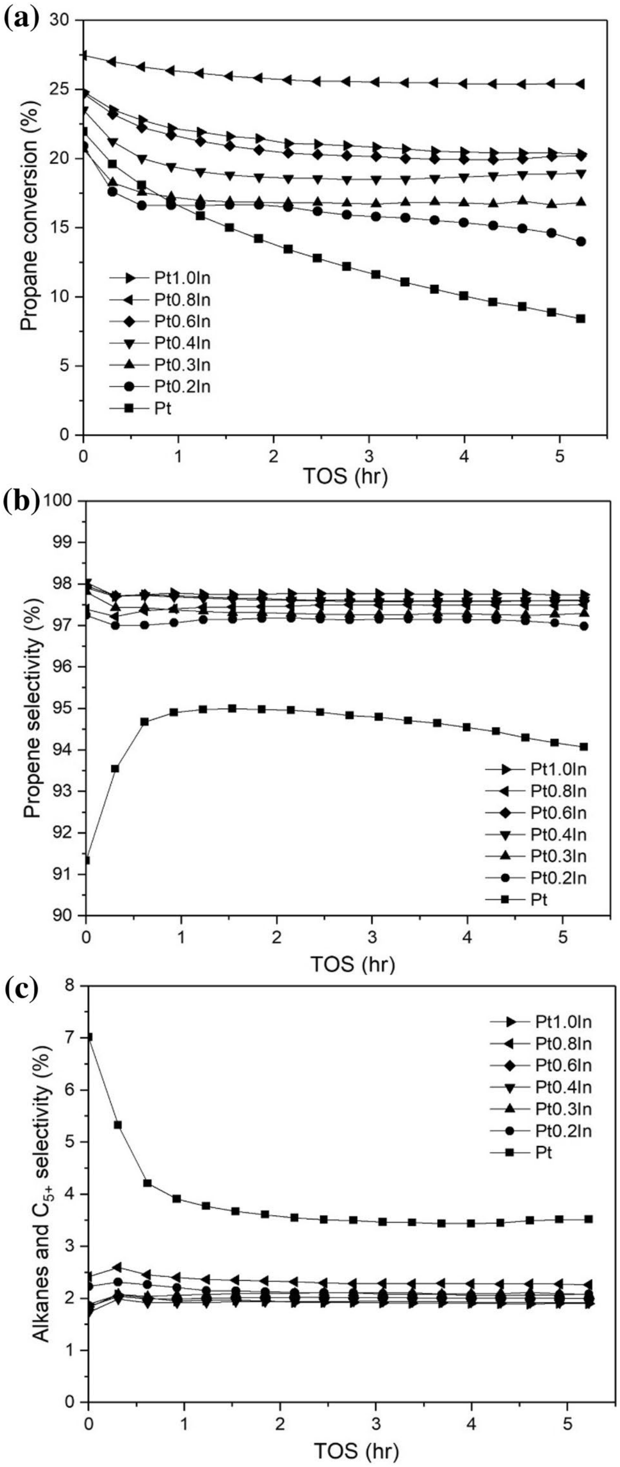

Fig. 1 (**a**) Conversion of propane, (**b**) selectivity to propene and (**c**) selectivity to alkanes and C_{5+} with respect to reaction time on the Pt*x*In with different In loadings ($x = 0.2–1.0$)

3.2 Characteristics of the PtxIn Catalysts

The acidic properties of the catalysts were investigated by NH_3-TPD and the results are displayed in Fig. 2. All the catalysts showed a similar appearance consisting of three desorption peak regions at (I) 130–138 °C, (II) 181–205 °C, and (III) 336–374 °C. Based on other PtIn/HT catalysts reported in the literature [27–29], these peaks could be inferred to weak and medium acid sites. A semi-quantitative comparison of the acid distribution was obtained by fitting the NH_3-TPD curves using the Gaussian deconvolution method and is summarized in Table 1. Addition of In by 0.2–1.0 wt% to the monometallic Pt catalyst slightly increased the sum of the total peak areas (~ 10%). However, the temperature of maximal peak intensity (T_M) for all the desorption peaks shifted to lower temperature for all the bimetallic PtIn catalysts especially for the higher temperature peak (peak III). The Pt0.8In exhibited the lowest T_M at 130, 181, and 336 °C. The shift of T_M observed in this study due to the effect of In loading was more pronounced comparing to those reported earlier on the effects of pH used in preparing Mg(Al)O, Mg/Al molar ratio, and the calcination temperature of the Mg(Al)O (T_M of each desorption range varied between 10 and 20 °C). The higher propene yield of the PtIn catalysts was correlated well with the lower acid strength of the bimetallic catalysts.

The effect of In loading on the reduction behaviors of catalysts was studied by H_2-TPR method. Figure 3 shows the TPR curves of Pt*x*In catalysts with different In loadings ($x = 0.2$–1.0 wt%). The monometallic Pt catalyst showed a low temperature reduction peak centered at 270 °C, which was assigned to the reduction of platinum species on the surface. The second peak located at 440 °C was assigned to the reduction of platinum species in the stronger interaction with support [33–35]. The first reduction peak slightly shifted towards lower temperature with increasing In loadings from 0.2 to 0.8 wt%. The hydrogen consumption was also decreased in a similar trend. Moreover, the hydrogen

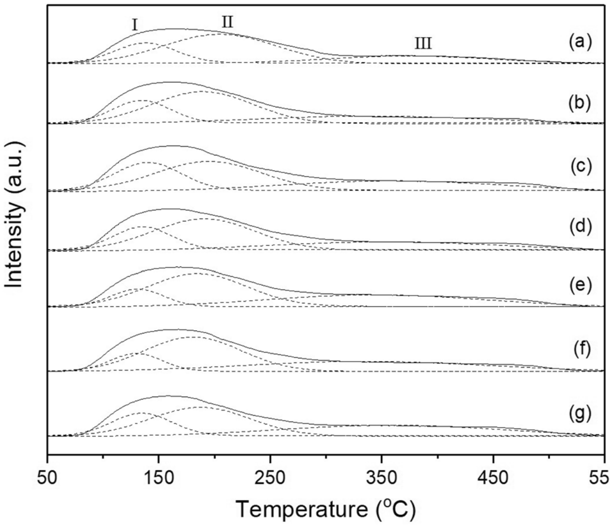

Fig. 2 NH_3-TPD profiles of Pt*x*In catalysts with different In loadings; (*a*) Pt, (*b*) Pt0.2In, (*c*) Pt0.3In, (*d*) Pt0.4In, (*e*) Pt0.6In, (*f*) Pt0.8In and (*g*) Pt1.0In

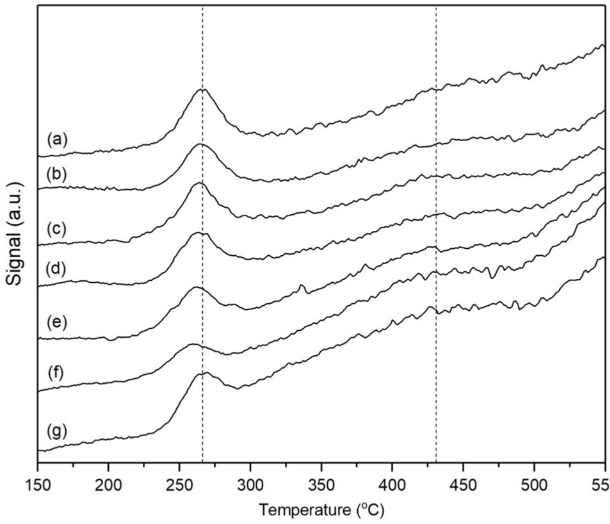

Fig. 3 H_2-TPR profiles of Pt*x*In catalysts with different In loadings; (*a*) Pt, (*b*) Pt0.2In, (*c*) Pt0.3In, (*d*) Pt0.4In, (*e*) Pt0.6In, (*f*) Pt0.8In and (*g*) Pt1.0In

Table 1 The semi-quantitative results of NH_3-TPD measurements

Catalysts	T_M (°C)			Total area (a.u.) (×10^2)	Peak area fraction (%)	
	I	II	III		I + II	III
Pt	138	205	374	8.1	79.4	20.6
Pt0.2In	135	189	340	8.3	71.8	28.2
Pt0.3In	138	195	355	9.0	66.8	33.3
Pt0.4In	136	191	350	8.9	66.6	33.4
Pt0.6In	131	186	344	9.0	63.7	36.3
Pt0.8In	130	181	336	8.8	63.2	36.8
Pt1.0In	135	187	357	8.9	62.7	37.3

consumption in the higher Pt reduction region was also increased as In loading increased for the bimetallic PtIn catalysts, which in agreement with the results of Jahel et al. [36]. It is worth mentioning that the hydrogen consumption in the region of Pt reduction increases as the In content increases. This indicates that a fraction of In initially being reduced with Pt at the temperature around 440 °C, possibly leading to the reduction of some In oxides into the metallic state. Such a shift of lower Pt reduction temperature and an increase of hydrogen consumption in higher Pt reduction region are typical of the close Pt–In intimacy, possibly in the form of PtIn alloys. However, for the case of Pt1.0In, a shift of lower Pt reduction temperature was not observed, thus the formation of PtIn was not clearly demonstrated.

Figure 4 shows the XPS spectra corresponding to In 3d$_{5/2}$ and In 3d$_{3/2}$ region of Pt0.6In, Pt0.8In, and Pt1.0In catalysts after reduction at 550 °C, respectively. After the deconvolution of the spectra, two In species were obtained at about 444.1–444.3 and 445.4–445.5 eV, corresponding to the different indium species. The lower binding energy was attributed to the formation of the zerovalent or metallic In [37–39], whereas the higher binding energy was ascribed to the oxidation state of In species on the surface of the catalysts. The deconvolution results of the corresponding spectra are summarized in Table 2, the percentages of the oxidation state of In species in Pt0.6In, Pt0.8In, and Pt1.0In catalysts were 64.7, 69.3, and 58.0%, respectively. The percentages of oxidation state of In species of Pt0.6In and Pt1.0In were distinctly lower than Pt0.8In catalyst, resulting in lower catalytic performance and stability. It was also observed that Pt1.0In with the highest amount of In loading showed the lowest fraction of the oxidation state of In species. According to previous studies [29, 30] indicated that a large fraction of metallic In could block Pt active sites, which may be a poison to the dehydrogenation reaction. These results verify that the suitable In loading can strengthen In–support interaction, stabilizing the oxidized In species. The excess amount of In loading can lead to large fraction of metallic In interacting strongly with Pt, which is disadvantageous to the propane dehydrogenation.

The TEM images of the catalysts and the corresponding particle size distributions of Pt, Pt0.8In and Pt1.0In catalysts are shown in Fig. 5. From Fig. 5a, it can be seen that the monometallic Pt particles were not well distributed on the support. Figure 5b illustrates more homogeneous distribution of metallic particles on the Pt0.8In catalyst and Fig. 5c displays a wide distribution of metallic particles size and poor dispersion of metallic particles for Pt1.0In. It is suggested that distribution of a suitable content of indium on the Pt catalyst is favorable to the more uniform distribution of bimetallic PtIn particles. The average metal particle size increased with increasing In loading from 0.63 nm (Pt) to 0.74 (Pt0.8In) and 0.91 nm (Pt1.0In). It is

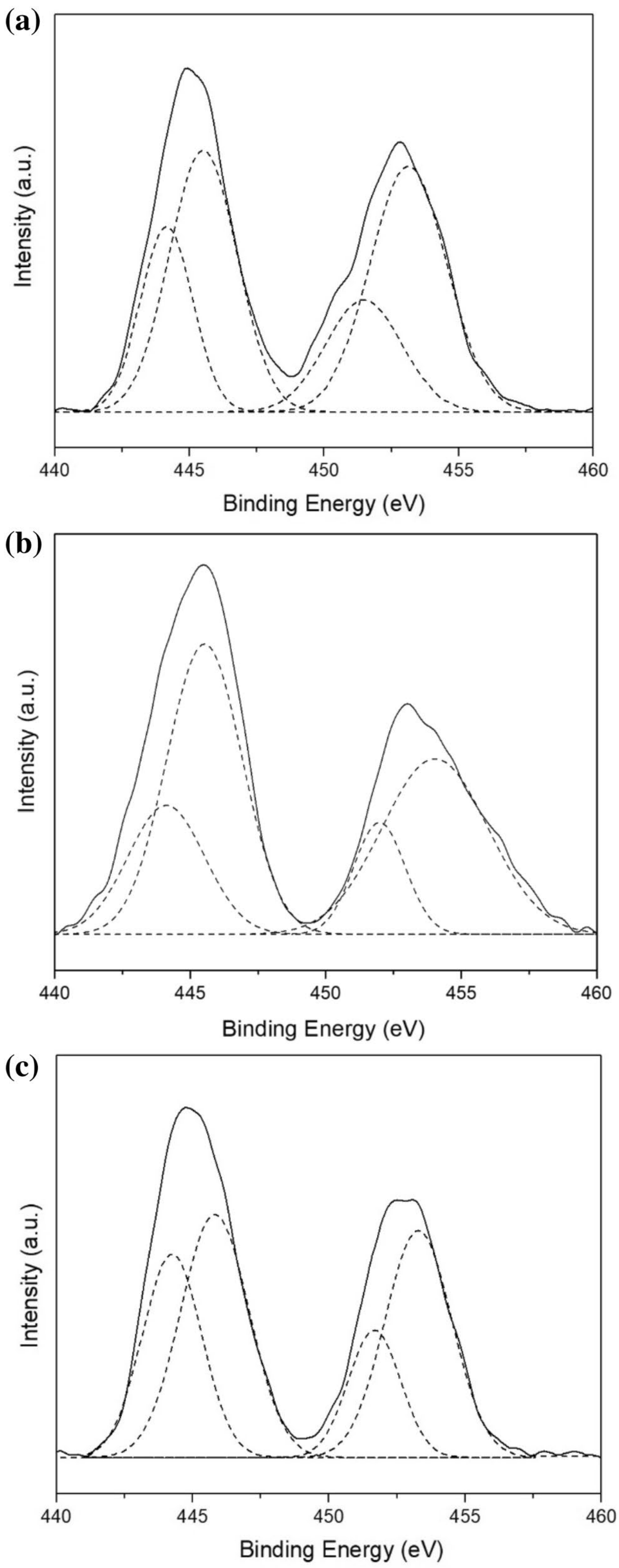

Fig. 4 In 3d XPS spectra of (**a**) Pt0.6In, (**b**) Pt0.8In and (**c**) Pt1.0In catalysts

Table 2 Summary of XPS results

Catalysts	Binding energy (eV)	
	In $3d_{5/2}$	In $3d_{3/2}$
Pt0.6In	444.2 (35.3%)	451.5 (31.3%)
	445.4 (64.7%)	453.1 (68.7%)
Pt0.8In	444.1 (30.7%)	452.6 (59.7%)
	445.4 (69.3%)	455.1 (40.3%)
Pt1.0In	444.3 (42.0%)	451.6 (35.9%)
	445.5 (58.0%)	453.2 (64.1%)

also suggested that addition of a suitable content of indium on the Pt catalyst (Pt0.8In) led to more uniform distribution of bimetallic PtIn particles.

Coking is an important factor for the deactivation of propane dehydrogenation catalysts. TPO was used to investigate the amount and nature of coke formed on the used catalysts. The typical TPO profiles of used catalysts are shown in Fig. 6. The used catalysts were collected after performed in the propane dehydrogenation at 550 °C for 5 h TOS. All the spent catalysts showed two successive peaks of carbon dioxide intensity representing two different carbon deposits. Generally, the first peak at low temperature located at around 264 °C are mainly to the carbon deposits that cover the active metal. The second peak at high temperature located at around 430 °C represents the carbon deposits that located on the external surface of the support [40]. Pt and Pt0.2In showed mainly combustion peak at about 430 °C with respect to high amount of coke on the support. It is clear that for the Pt catalyst, coke deposits cover on active sites and mainly on the support, corresponding to quick deactivation. When In loading was increased from 0.2 to 1.0 wt%, the combustion peaks at about 264 and 430 °C shifted to lower temperature of 247 and 385 °C, respectively and strongly decrease of coke amount at the high combustion peak was also observed. The coke amount decreased with increasing In loading to 1.0 wt% with Pt0.8In showed the lowest coke amount corresponding to the highest catalytic performance. The TPO result reveals that coke formation on the support is the main factor for catalyst deactivation over the PtIn catalysts. It has been also reported that most of carbon deposits cover on the active metal and coke formation is related to the olefin absorption behavior on the active sites [40–42]. According to the previous study by Sun et al. [31], it was observed that alloying of Pt with In greatly reduced the amount of coke deposited of ethane and propane dehydrogenation. Therefore, the result suggests that addition of In on Pt catalyst significantly lowered the amount of coke formation, particularly on the support, resulting in high catalyst stability.

4 Conclusions

In this study, the Pt–In catalysts supported on a commercially available Mg(Al)O support were prepared with 0.3 wt% Pt and various In loadings from 0.2 to 1.0 wt%. It is found that the addition of In to the monometallic Pt catalyst could reduce the acidity strength especially the strong acid site. The TPR and XPS measurements verified that the introduction of In in the range of 0.2–0.8 wt% by impregnation on the Pt/Mg(Al)O catalyst led to metallic In and PtIn alloy formation and improved catalytic performances for propane dehydrogenation. However, excessive amount of In (i.e., 1.0 wt%) resulted in larger fraction of metallic state (In^0), which is disadvantageous to the propane dehydrogenation. All the PtIn/Mg(Al)O catalysts exhibited higher propane conversion and lower amount of coke deposited, compared to the Pt/Mg(Al)O. The best catalytic performances for propane dehydrogenation were obtained on the Pt0.8In catalyst exhibits with ≥ 97.5% propylene selectivity and 27.5% yield at 550 °C and 5 h TOS.

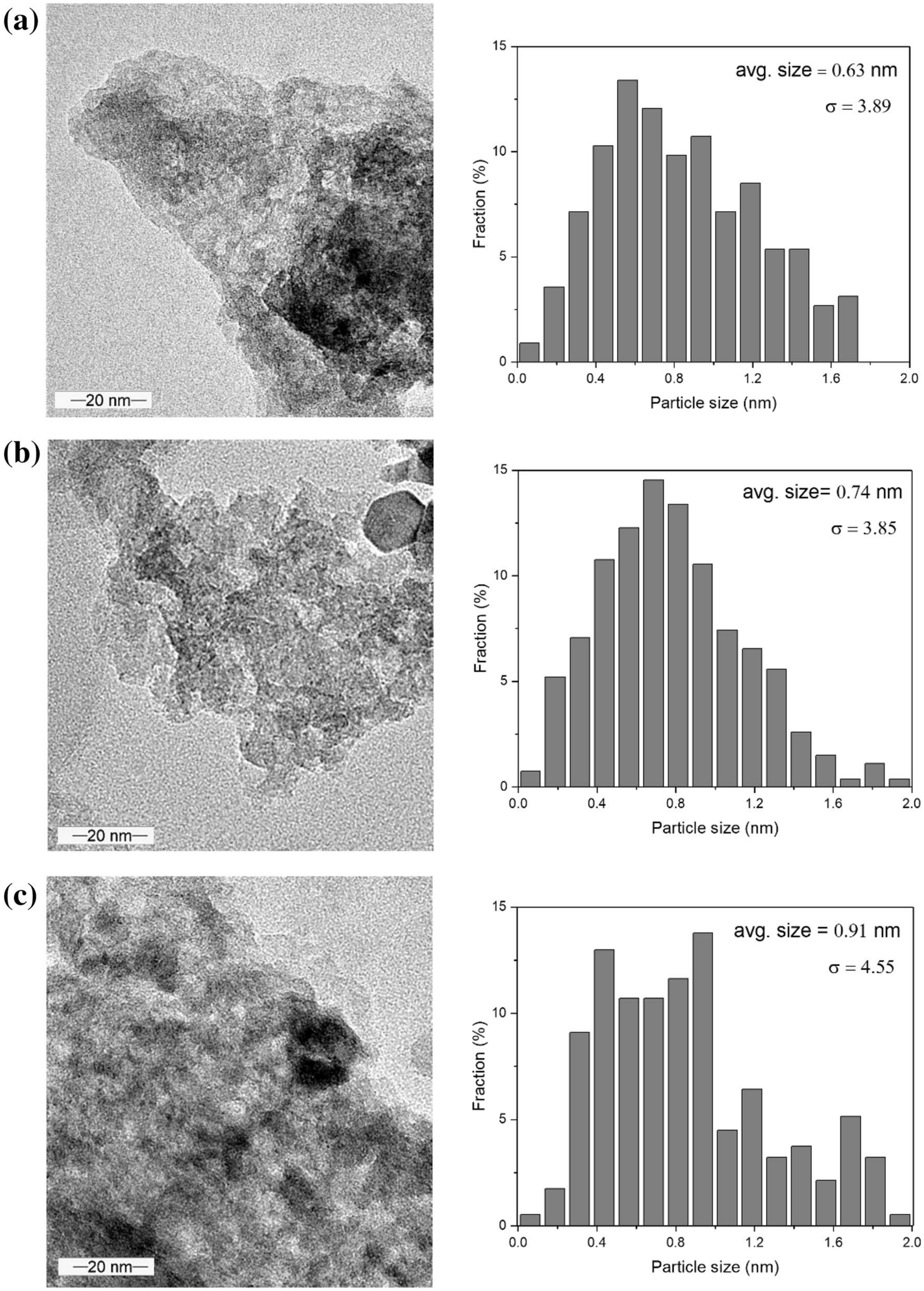

Fig. 5 TEM micrographs and particle size distributions of (**a**) Pt, (**b**) Pt0.8In and (**c**) Pt1.0In catalysts

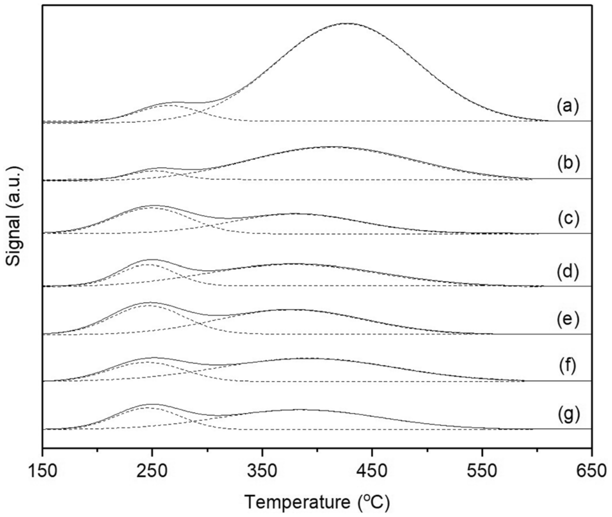

Fig. 6 TPO profiles of used Pt*x*In catalysts with different In loadings; (*a*) Pt, (*b*) Pt0.2In, (*c*) Pt0.3In, (*d*) Pt0.4In, (*e*) Pt0.6In, (*f*) Pt0.8In and (*g*) Pt1.0In

Acknowledgements The authors would like to thank SCG Chemical Co., Ltd. for the scholarship for W.T., the financial supports, and research facilities provided. The financial support from the Thailand Research Fund is also gratefully acknowledged.

References

1. Fattahi M et al (2011) The effect of oxygenate additives on the performance of Pt–Sn/γ-Al_2O_3 catalyst in the propane dehydrogenation process. Sci Iran 18(6):1377–1383
2. Zhang Y et al (2006) Effect of alumina binder on catalytic performance of PtSnNa/ZSM-5 catalyst for propane dehydrogenation. Ind Eng Chem Res 45(7):2213–2219
3. Long L-L et al (2014) Improved catalytic stability of PtSnIn/xCa–Al catalysts for propane dehydrogenation to propylene. Chem Eng J 257(0):209–217
4. Serrano-Ruiz JC, Sepúlveda-Escribano A, Rodríguez-Reinoso F (2007) Bimetallic PtSn/C catalysts promoted by ceria: application in the nonoxidative dehydrogenation of isobutane. J Catal 246(1):158–165
5. Wu J et al (2014) n-Butane dehydrogenation over Pt/Mg(In)(Al)O. Appl Catal A 470(0):208–214
6. Praserthdam P, Grisdanurak N, Yuangsawatdikul W (2000) Coke formation over Pt–Sn–K/Al_2O_3 in C3, C5–C8 alkane dehydrogenation. Chem Eng J 77(3):215–219
7. Llorca J et al (1999) Supported Pt–Sn catalysts highly selective for isobutane dehydrogenation: preparation, characterization and catalytic behavior. Appl Catal A 189(1):77–86
8. Stagg SM et al (1997) Isobutane dehydrogenation on Pt–Sn/SiO_2 catalysts: effect of preparation variables and regeneration treatments. J Catal 168:75–94
9. Sahebdelfar S et al (2011) Modeling of adiabatic moving-bed reactor for dehydrogenation of isobutane to isobutene. Appl Catal A 395(1):107–113
10. Lobera MP et al (2008) Propane dehydrogenation over Pt–Sn–K/γ-Al_2O_3 catalyst in a two-zone fluidized bed reactor. Ind Eng Chem Res 47(23):9314–9320
11. Wan L et al (2011) Influence of lanthanum addition on catalytic properties of PtSnK/Al_2O_3 catalyst for isobutane dehydrogenation. Ind Eng Chem Res 50(8):4280–4285
12. de Graaf EA et al (2005) Pt0.02Sn0.003Mg0.06 on γ-alumina: a stable catalyst for oxidative dehydrogenation of ethane. Appl Catal A 278(2):187–194
13. Ahmad I et al (2016) La–Sn oxide nanocatalyst: efficient materials for the synthesis of cyclohexanones. J Mol Liq 224(Part A):359–365
14. Homs Ns et al (2003) Silica-supported PtSn alloy doped with Ga, In or, Tl: characterization and catalytic behaviour in n-hexane dehydrogenation. J Mol Catal A 200(1):251–259
15. Jablonski EL et al (1999) Effect of Ga addition to Pt/Al_2O_3 on the activity, selectivity and deactivation in the propane dehydrogenation. Appl Catal A 183(1):189–198
16. Pakhomov NA (2001) Reversible and irreversible deactivation of supported bimetallic catalysts for the dehydrogenation of lower paraffins. Kinet Catal 42(3):334–343
17. Castro AA (1993) Catalysts for the selective dehydrogenation of high molecular weight paraffins. Catal Lett 22(1):123–133
18. Sun P et al (2010) Synthesis and characterization of a new catalyst Pt/Mg(Ga)(Al)O for alkane dehydrogenation. J Catal 274(2):192–199
19. Passos FB, Aranda DAG, Schmal M (1998) Characterization and catalytic activity of bimetallic Pt-In/Al_2O_3 and Pt-Sn/Al_2O_3 catalysts. J Catal 178(2):478–488
20. Galvita V et al (2010) Ethane dehydrogenation on Pt/Mg(Al)O and PtSn/Mg(Al)O catalysts. J Catal 271(2):209–219
21. Wu J, Peng Z, Bell AT (2014) Effects of composition and metal particle size on ethane dehydrogenation over PtxSn100–x/Mg(Al)O ($70 \leq x \leq 100$). J Catal 311:161–168
22. Akporiaye D et al (2001) A novel, highly efficient catalyst for propane dehydrogenation. Ind Eng Chem Res 40(22):4741–4748
23. Virnovskaia A et al (2007) Characterization of Pt,Sn/Mg(Al)O catalysts for light alkane dehydrogenation by FT-IR spectroscopy and catalytic measurements. J Phys Chem C 111(40):14732–14742
24. Wu J et al (2015) Ethane and propane dehydrogenation over PtIr/Mg(Al)O. Appl Catal A 506:25–32
25. Cortright RD, Hill JM, Dumesic JA (2000) Selective dehydrogenation of isobutane over supported Pt/Sn catalysts. Catal Today 55(3):213–223
26. de Miguel S et al (1996) FTIR and XPS study of supported PtSn catalysts used for light paraffins dehydrogenation. Catal Lett 36(3):201–206
27. Shen L-L et al (2017) The effects of calcination temperature of support on PtIn/Mg(Al)O catalysts for propane dehydrogenation reaction. Chem Eng J 324(Supplement C):336–346
28. Xia K et al (2016) The properties and catalytic performance of PtIn/Mg(Al)O catalysts for the propane dehydrogenation reaction: effects of pH value in preparing Mg(Al)O supports by the co-precipitation method. J Catal 338:104–114
29. Xia K et al (2016) The influences of Mg/Al molar ratio on the properties of PtIn/Mg(Al)O-x catalysts for propane dehydrogenation reaction. Chem Eng J 284:1068–1079
30. Xia K et al (2015) Analysis of the catalytic activity induction and deactivation of PtIn/Mg(Al)O catalysts for propane dehydrogenation reaction. RSC Adv 5(79):64689–64695
31. Sun P et al (2011) Novel Pt/Mg(In)(Al)O catalysts for ethane and propane dehydrogenation. J Catal 282(1):165–174
32. Sattler JJHB et al (2014) Catalytic dehydrogenation of light alkanes on metals and metal oxides. Chem Rev 114(20):10613–10653

33. De Miguel SR et al (1988) Platinum—tin/alumina catalyst: modification of the metallic phase after successive oxidation—reduction cycles. Appl Catal 45(1):61–69
34. Thomas R et al (1980) On the formation of aluminum tungstate and its presence in tungsten oxide on γ-alumina catalysts. J Catal 61(2):559–561
35. Lieske H et al (1983) Reactions of platinum in oxygen- and hydrogen-treated Ptγ-Al_2O_3 catalysts: I. Temperature-programmed reduction, adsorption, and redispersion of platinum. J Catal 81(1):8–16
36. Jahel A et al (2010) Effect of indium in trimetallic Pt/Al_2O_3SnIn–Cl naphtha-reforming catalysts. J Catal 272(2):275–286
37. Hewitt RW, Winograd N (1980) Oxidation of polycrystalline indium studied by X-ray photoelectron spectroscopy and static secondary ion mass spectroscopy. J Appl Phys 51(5):2620–2624
38. Hollinger G, Skheyta-Kabbani R, Gendry M (1994) Oxides on GaAs and InAs surfaces: an X-ray-photoelectron-spectroscopy study of reference compounds and thin oxide layers. Phys Rev B 49(16):11159–11167
39. Wagner CD (1975) Chemical shifts of Auger lines, and the Auger parameter. Faraday Discuss Chem Soc 60(0):291–300
40. Zhang Y et al (2013) Propane dehydrogenation over PtSnNa/La-doped Al_2O_3 catalyst: effect of La content. Fuel Process Technol 111:94–104
41. Zhang Y et al (2011) Effect of magnesium addition on catalytic performance of PtSnK/γ-Al_2O_3 catalyst for isobutane dehydrogenation. Fuel Process Technol 92(8):1632–1638
42. Zhang Y et al (2011) Synergistic effect between Sn and K promoters on supported platinum catalyst for isobutane dehydrogenation. J Nat Gas Chem 20(6):639–646